Development of a metalloproteomic approach to analyse the response of Arabidopsis cells to uranium stress

Manon Sarthou, Benoît Revel, Florent Villiers, Claude Alban, Titouan Bonnot, Océane Gigarel, Anne-Marie Boisson, Stephane Ravanel, Jacques Bourguignon

Metallomics

Integrated biometal science

Accepted Manuscript

This article can be cited before page numbers have been issued, to do this please use: M. Sarthou, B. Revel, F. Villiers, C. Alban, T. Bonnot, O. Gigarel, A. Boisson, S. Ravanel and J. Bourguignon, *Metallomics*, 2020, DOI: 10.1039/D0MT00092B.

ROYAL SOCIETY OF CHEMISTRY

rsc.li/metallomics

Development of a metalloproteomic approach to analyse the response of Arabidopsis cells to uranium stress

Manon Sarthou†, Benoit Revel†, Florent Villiers†[a], Claude Alban, Titouan Bonnot[b], Océane Gigarel, Anne-Marie Boisson, Stéphane Ravanel and Jacques Bourguignon

†MS, BR and FV contributed equally to this work

[a]Present address: Bayer Crops Science, Lyon, La Dagoire, France

[b]Present address: Department of Botany and Plant Sciences, University of California, Riverside, 92507 Riverside, USA

Univ. Grenoble Alpes, CEA, INRAE, CNRS, IRIG, LPCV, 38000 Grenoble, France

Financial source

This work was funded by grants from the CEA Toxicology Programme and from the Agence Nationale de la Recherche (ANR-17-CE34-0007, GreenU project; ANR-10-LABX-49-01, Labex GRAL; ANR-17-EURE-0003, CBH-EUR-GS).

Correspondance:

Jacques Bourguignon, Univ. Grenoble Alpes, CEA, CNRS, INRAE, IRIG, LPCV, 17 avenue des Martyrs, 38000 Grenoble, France. +33 438784688
jacques.bourguignon@cea.fr

Stéphane Ravanel, Univ. Grenoble Alpes, INRAE, CEA, CNRS, IRIG, LPCV, 17 avenue des Martyrs, 38000 Grenoble, France. +33 438783383
stephane.ravanel@cea.fr

Key words: ionome, ionoproteomics, metalloproteomics, post-translational modification, protein methylation, uranium.

Abstract

Uranium is a naturally occurring radionuclide that is absorbed by plants and interferes with many aspects of their physiology and development. In this study, we used an ionomic, metalloproteomic, and biochemical approach to gain insights into the impact of uranyl on the proteome of *Arabidopsis thaliana* cells. First, we showed that most of U was trapped in the cell wall and only a small part of the radionuclide was found in the cell soluble fraction. Also, the homeostasis of several essential elements was significantly modified in cells challenged with U. Second, the soluble proteome from Arabidopsis cells was fractionated into 10 subproteomes using anion-exchange chromatography. Proteomic analyses identified 3676 proteins in the different subproteomes and metal-binding proteins were profiled using inductively coupled plasma mass spectrometry. Uranium was detected in several chromatographic fractions, indicating for the first time that several pools of Arabidopsis proteins are capable to bind uranyl *in vivo*. Third, we showed that the pattern of some lysine and arginine methylated proteins was modified following exposure to U. We further identified that the ribosomal protein RPS10C was dimethylated at two arginine residues in response to uranyl stress. Together, these results provide the first clues on the impact of U on the Arabidopsis proteome and pave the way for the future identification of U-binding proteins.

Significance to Metallomics statement

Knowledge of the mechanisms of metal toxicity depends largely on understanding the impact of metals on cellular proteins. The development of ionomic, proteomic, metalloproteomic, and biochemical approaches is essential to reach this objective. Here, we used this strategy to gain insight into the consequences of uranyl exposure on the proteome of *Arabidopsis thaliana* cells. The inventory of native Arabidopsis proteins fractionated by anion-exchange chromatography, together with their biochemical properties and coelution with metals, provides a unique tool for targeted biochemical characterization, including the analysis of metal-binding proteins, post-translational modifications, or protein complexes.

Introduction

Uranium (U) is a non-essential trace metal element that is ubiquitous in the Earth crust, with average worldwide concentrations of 3 ppm (mg/kg) in soil and 3 ppb (µg/L) in sea water. The radionuclide is primarily redistributed in the environment by anthropogenic activities related to U mining and milling industries, civil and military nuclear activities, and extensive enrichment of agricultural soils with phosphate fertilizers, which may be significantly contaminated with U.[1-3] The accumulation of U in soil, water and air can lead to potential risks to ecosystems, agrosystems, and ultimately human health, as the radionuclide has both chemical and radiological effects. Natural U is of low radiotoxicity due to its isotopic composition (>99% ^{238}U) but the uranyl ion (UO_2^{2+}) that is prevalent in oxidizing environments is highly chemotoxic for all living organisms.[4] As predicted by the hard and soft acids and bases principle,[5] UO_2^{2+} is a hard acid that reacts preferentially with hard oxygen donors such as phosphate, carboxylate, carbonate and hydroxyl groups, mainly through electrostatic interactions. Therefore, the biological ligands of U can be very diverse, including metabolites, proteins or peptides.[6] The identification of molecular targets of uranyl is an essential step in understanding the mechanisms of radionuclide toxicity, and possibly detoxification, in a given organism.

Uranium is absorbed by plants and interferes with many aspects of their physiology and development.[7-11] Uranium inhibits plant growth, modifies root growth and architecture, disrupts mineral nutrition and homeostasis, and affects photosynthesis.[12-19] At the cellular level, U induces nitric oxide and hydrogen peroxide production and triggers defence mechanisms against oxidative stress.[19,20] Also, U perturbs iron, phosphate and manganese homeostasis [9,14,21,22] and triggers important changes in the metabolome.[23] At the molecular level, U has been shown to alter the expression of genes involved in iron and phosphate homeostasis, hormone synthesis and signalling, and cell wall metabolism in *Arabidopsis thaliana.*[21] *Vicia faba* plants challenged with U also displayed important changes of their transcriptome.[23] Despite these studies, the consequences of uranyl on the dynamics of proteomes and the molecular targets of U are still not known in plants. Since uranyl is able to bind strongly to biomolecules via carboxylate, phosphate or sulphate moieties, proteins are expected to be the primary targets of U. The most relevant strategy for the identification of uranyl-protein complexes formed *in vivo* is a metalloproteomic approach combining efficient protein

separation techniques that preserve uranyl-protein interactions with powerful protein and metal identification systems, i.e. protein tandem mass spectrometry (MS/MS) and inductively coupled plasma mass spectrometry (ICP-MS), respectively.[24,25]

Metalloproteins account for more than a third of total proteins and are involved in a wide array of functions related to the functional, structural and regulatory roles of bound metals.[26,27] The main challenge in the identification of metalloproteins by using top-down proteomic approaches is to preserve non-covalent and labile metal-protein complexes during protein fractionation steps.[25] Metalloproteomic studies in plants are scarce and, thus, plant iono- or metallo-proteomes are largely uncharacterized. A few studies describe the identification of copper-binding proteins in Arabidopsis roots,[28] and copper-, zinc- and cobalt-binding proteins from Arabidopsis mitochondria[29] using immobilized metal affinity chromatography (IMAC). To our knowledge, the proteome-wide identification of true native metal-binding proteins, and not proteins that are able to bind metals *in vitro* as identified by IMAC strategies, has never been done in plants. In contrast, such studies have been performed in microorganisms[24,30,31] or human cells such as primary neuron and astrocytes culture.[32] These studies used a combination of non-denaturing electrophoretic and/or chromatographic steps combined with ICP-MS analyses and identified a large array of proteins that bind essentials and non-essential elements. *In vivo* identification of potential U-binding proteins has been described in the Archaea *Pyrococcus furiosus*[30], the crayfish species *Procambarus clarkia*,[33] zebrafish,[34] and human dopaminergic cells[35] challenged with the radionuclide. The identified U-binding proteins are involved in iron homeostasis (e.g. ferritin), carbohydrate metabolism, oxidative stress regulation, cytoskeleton, or protein ubiquitination.

In the present study, we developed an ionomic, top-down proteomic, and biochemical approach to gain insights into the impact of uranyl on the proteome of *Arabidopsis thaliana* cells. First, we showed that Arabidopsis cells challenged with U displayed significant changes in the homeostasis of essential elements and that only a small part of the radionuclide was retrieved in the cell soluble fraction. Second, the soluble proteome from Arabidopsis cells was fractionated into 10 subproteomes using anion-exchange chromatography that allowed a reduction of sample complexity. Proteomic analyses identified 3676 proteins in the different subproteomes and metal-binding proteins were profiled using ICP-MS. Uranium was detected in several chromatographic fractions, indicating for the first time that a number of Arabidopsis

proteins are able to bind U *in vivo*. Third, we analysed the consequences of U stress on the expression patterns of lysine (Lys) and arginine (Arg) methylated proteins. We identified an Arg methylated protein involved in translation that is highly methylated in response to U stress. Together, these results show for the first time the consequences of U on the Arabidopsis proteome and pave the way for the future purification and identification of U-binding proteins in Arabidopsis.

Methods

Arabidopsis cells growth conditions

Arabidopsis thaliana (ecotype Columbia) cells in suspension cultures were grown under continuous light (40 µmol of photons m^{-2} s^{-1}) at 22°C with rotary agitation at 125 rpm in Murashige and Skoog (MS) medium supplemented with 1.5% (w/v) sucrose. Cells were subcultured every 4 days for 3 cycles before being challenged with U. To this aim, exponentially growing cells were harvested by centrifugation, washed once and re-suspended in MS medium with low phosphate content, 30 µM KH_2PO_4 instead of 1.25 mM in regular MS. Cells (about 10 g fresh weight in 200 mL of medium) were challenged with 50 µM uranyl nitrate or maintained in MS low Pi for 24 h before harvesting. The incubation period is sufficient to allow cells to adsorb almost all of the radionuclide from the medium while preserving cellular integrity. Cells were washed once in 10 mM Na_2CO_3, then twice in distilled water, and dried by vacuum filtration using a Buchner funnel. Cells were used immediately or stored at -80°C for further analyses.

Preparation of protoplasts and soluble fractions

Freshly harvested cells (about 1 g) were used to prepare protoplasts by enzymatic digestion of cell walls. Cells were suspended in 1.5 mL of digestion buffer [(2%(w/v) cellulase (Onozuka R-10, Fisher Scientific), 0.5% (w/v) pectolyase (Y-23, Fisher Scientific), 0.6 M mannitol, 25 mM MES, pH 5.5] and incubated at 28°C with rotary agitation at 120 rpm until protoplasts were released. Protoplasts were harvested by filtration through a 78-µm nylon mesh, diluted 10-fold in washing buffer (0.7 M mannitol, 15 mM MES, 10 mM Tris, pH 7.0), and centrifuged at 100xg for 5 min. Protoplasts were washed twice in the same buffer to remove any trace of digestion enzymes. A fraction

View Article Online
DOI: 10.1039/D0MT00092B

of protoplasts was lysed by osmotic shock following resuspension in 10 mM Tris, pH 7.0, and three cycles of freezing (liquid nitrogen) and thawing (water bath at 30°C). Protoplast soluble fractions were recovered by ultracentrifugation at 105,000xg for 20 min.

Preparation of protein extracts and fractionation

Total soluble proteins from cultured cells were extracted by grinding powdered samples in 10 mM Tris-HCl, pH 7.5, 1 mM dithiothreitol, and a cocktail of protease inhibitors (Roche Applied Science, ref 04693132001). Samples were centrifuged at 16,000 x g for 20 min at 4°C and the supernatant used as a source of soluble proteins. After desalting on PD10 Sephadex G25 (M) columns (GE Healthcare), soluble proteins were fractionated by chromatography onto Q-Sepharose High Performance (GE Healthcare) columns (1.6 x 5 cm) equilibrated with the extraction buffer, and stepwise elution using discontinuous increasing NaCl concentrations in the same buffer (from 0 to 1 M NaCl). Collected fractions were stored at -80°C until used for further analyses.

Protein determination and immunoblotting analyses

Proteins were measured by the Bradford method using Bio-Rad protein assay reagent, with BSA as a standard.[36] Protein fraction aliquots (30 µg) were concentrated by precipitation with 10% (v/v) trichloroacetic acid, resolved by SDS-PAGE, and either stained with Coomassie Brilliant Blue R250 or electroblotted to nitrocellulose membranes, and probed using rabbit polyclonal antibodies to trimethylated lysine (ab76118, abcam) or to asymmetric dimethyl arginine (adme-R, Cell Signaling Technology). Protein detection was achieved using the ECL Plus™ Western Blotting detection reagents and a Typhoon 9400 scanner (Amersham Biosciences).

Mass spectrometry analyses

Protein identification in the Q-Sepharose fractions - Proteins contained in each fraction were concentrated in the top of a SDS-PAGE and stained with Coomassie blue. Proteins were treated in gel with dithiothreitol and iodoacetamide before digestion using trypsin. The resulting peptides were extracted and analysed by online nanoLC-MS/MS (UltiMate 3000 and LTQ-Orbitrap Velos, Thermo Scientific) using a 120-min gradient. For this, peptides were sampled on a 300 µm x 5 mm PepMap C18 precolumn and separated on a 75 µm x 150 mm PepMap C18 column (Thermo Scientific). MS

and MS/MS data were acquired using Xcalibur (Thermo Scientific). Mascot Distiller (Matrix Science) was used to produce mgf files before identification of peptides and proteins using Mascot (version 2.3) through concomitant searches against TAIR (version 10), classical contaminants database (homemade), and the corresponding reversed databases. ESI-TRAP was chosen as the instrument, trypsin/P as the enzyme, and 2 missed cleavage allowed. Precursor and fragment mass error tolerances were set respectively at 10 ppm and 0.6 Da. Peptide modifications allowed during the search were: carbamidomethyl (C, fixed) acetyl (protein N-terminus, variable) and oxidation (M, variable). The IRMa software[37] was used to filter the results: conservation of rank 1 peptides, peptide identification FDR < 1% (as calculated by employing the reverse database strategy), and minimum of 1 specific peptide per identified protein group. The filtered results were uploaded into a relational mass spectrometry identification database and hEIDI[38] was used for the compilation, grouping and comparison of the protein groups from the different samples.

Analysis of post-translational modifications in Arabidopsis cells exposed to U stress - Protein bands were cut out before in-gel treatment with dithiothreitol and iodoacetamide and digestion with trypsin. The resulting peptides were extracted and analysed by online nanoLC-MS/MS (UltiMate 3000 RSLCnano and Q-Exactive Plus, Thermo Scientific) using a 40-min gradient. For this, peptides were sampled on a 300 µm x 5 mm PepMap C18 precolumn (Thermo Scientific) and separated on a 75 µm x 250 mm C18 column (Reprosil-Pur 120 C18-AQ, 1.9 µm, Dr. Maisch). MS and MS/MS data were acquired using Xcalibur (Thermo Scientific). RAW files were processed using MaxQuant[39] version 1.5.5.1. Spectra were searched against the Uniprot database (*Arabidopsis thaliana* taxonomy, December 2016 version), the frequently observed contaminants database embedded in MaxQuant, and the corresponding reversed databases. Trypsin was chosen as the enzyme and two missed cleavages were allowed. Precursor and fragment mass error tolerances were set at their default values. Peptide modifications allowed during the search were: carbamidomethyl (C, fixed), acetyl (protein N-terminus, variable), oxidation (M, variable), methyl (KR, variable) and dimethyl (KR, variable). Minimum number of peptides, razor + unique peptides, and unique peptides were set to 1. Maximum false discovery rates were set to 0.01 at peptide, protein and site levels. The match between runs option was activated.

ICP-MS analyses

Cells, protoplasts, and soluble fractions were digested at 90°C for 4 hours in 65% (w/v) HNO_3 (Suprapur, Merck). Protein fractions from AEC were incubated with 10% (v/v) HNO_3 for 2h at 55°C to ensure denaturation and release of bound elements. Denatured proteins were removed by centrifugation and the supernatants use for ICP-MS analysis. Mineralized samples were diluted in 0.5% (v/v) HNO_3 and analysed using an iCAP RQ quadrupole mass instrument (Thermo Fisher Scientific GmbH, Germany) equipped with a MicroMist U-Series glass concentric nebulizer, a quartz spray chamber cooled at 3°C, a Qnova quartz torch, a nickel sample cone, a nickel skimmer cone with a high-sensitivity insert, and an ASX-560 autosampler (Teledyne CETAC Technologies, USA). Elements were analysed using either the standard mode (for ^{24}Mg, ^{25}Mg, ^{39}K, ^{43}Ca, ^{44}Ca, ^{95}Mo, ^{98}Mo, and ^{238}U) or the kinetic energy discrimination mode with helium as the collision cell gas (for ^{55}Mn, ^{56}Fe, ^{57}Fe, ^{63}Cu, ^{65}Cu, ^{64}Zn, ^{66}Zn). Concentrations were determined using standard curves and corrected using an internal standard solution containing ^{103}Rh and ^{172}Y added online. Data integration was done using the Qtegra software (Thermo Fisher Scientific GmbH, Germany).

Results and discussion

Ionomic analysis of Arabidopsis cells challenged with uranium

We analysed the ionome of *Arabidopsis thaliana* cell suspension cultures challenged with U. Cells growing exponentially in a standard MS medium were transferred into a MS medium with low phosphate content (30 µM instead of 1.25 mM) supplemented or not with 50 µM uranyl nitrate. Low phosphate conditions have been used to limit the interaction between U and phosphate that is limiting the bioavailability of the radionuclide.[9,22] Cells were harvested after 24 h of U stress and extensively washed with Na_2CO_3 and distilled water to remove elements that are loosely adsorbed to the cell surface. Protoplasts were isolated from freshly harvested cells following cell wall digestion and further lysed by osmotic shock and ultracentrifuged to recover soluble fractions. Each fraction (whole cells, protoplasts, soluble fractions) was mineralized in nitric acid and analysed by ICP-MS to determine the effect of U on the ionome of Arabidopsis cells (Table 1). Potassium (K), magnesium (Mg), and calcium (Ca) were the most abundant elements measured in Arabidopsis cells, followed by iron (Fe), zinc

View Article Online
DOI: 10.1039/D0MT00092B

(Zn), manganese (Mn), molybdenum (Mo), and copper (Cu). After 24 h of treatment with uranyl nitrate, the amount of U in cells was 7±2 µg.mg^{-1} protein, which is an intermediate value between the amount of macro- and micro-elements. Uranium triggered a significant decrease in the amount of Fe (27%) and K (11%) in Arabidopsis cells but did not changed the other elements (Table 1). In protoplasts, the amount of U was 2.7±0.5 µg.mg^{-1} protein, which is about 5-time higher than the most abundant micro-elements Fe and Zn. However, the effect of U treatment on ion homeostasis in protoplasts was significant only for K (25% decrease) and Mg (14% decrease) (Table 1). Elemental analyses in whole cells and protoplasts allowed us to calculate the distribution of U and other elements between the cell wall and the protoplast, assuming that cell wall proteins account for 0.5 to 6% of total cellular proteins.[40] This calculation showed that 65% of U was present in the cell wall (Fig. 1). A similar distribution was observed for Mg, Mn, Fe, Zn, and Mo. Potassium was also mainly present in the cell wall (about 80-90%) whereas 80-90% of the pools of Ca and Cu were associated with the protoplast (Fig. 1). These results suggested that the cell wall is a major site for the storage of several essential elements as well as U, at least in cultured Arabidopsis cells. In the soluble fractions of protoplasts the amount of U was low (0.10±0.05 µg.mg^{-1} protein) (Table 1), indicating that in protoplasts most of the radionuclide was associated with membranes or with molecules forming complexes or precipitates eliminated by ultracentrifugation. In addition, the amount of Mn, Zn and Mg was significantly reduced (22, 19, and 16%, respectively) in the soluble fraction of Arabidopsis protoplasts upon U stress (Table 1). One cannot exclude that a small part of U measured in the cell soluble fraction was due to elemental redistribution during the fractionation procedure. However, the identification of U-enriched protein fractions by anion exchange chromatography (see below) supports the formation of U-protein complexes *in cellulo* following the incorporation of the radionuclide within Arabidopsis cell. Together, these data indicated that, despite the existence of important barriers for the uptake of U (cell wall, membranes and putative chelators), a limited amount of the toxic element has reached the soluble phase of Arabidopsis cells, where it can probably interact with soluble protein targets.

Fractionation of the soluble proteome from Arabidopsis cells

A key step towards the identification of proteins interacting with U is the fractionation of the soluble proteome while preserving the labile protein-metal interaction.[30,33-35] To

this aim the soluble proteome prepared from Arabidopsis cultured cells was resolved by anion exchange chromatography (AEC) using a High Performance Q-Sepharose column. A sodium chloride step gradient was set up to obtain a homogenous distribution of the amount of proteins in each fraction (Fig. 2A). The Arabidopsis cell proteome was separated into ten fractions corresponding to the flow through (fraction F0) and nine fractions corresponding to proteins eluted at 50, 100, 150, 200, 250, 300, 350, 400, and 1000 mM NaCl (fractions F50 to F1000, respectively). For both control and U-treated Arabidopsis cells, the fractionation procedure allowed to reduce the complexity of the protein samples in a highly reproducible manner and to enrich low-abundant proteins (Fig. 2).

Identification of proteins in the 10 sub-proteomes from Arabidopsis cells by LC-MS/MS

We used three of the four replicate experiments of fractionation (Fig. 2B) to identify the proteins present in each of the fractions resolved by AEC. Using LC-MS/MS a total of 6603 proteins were identified by shotgun proteomics in the 10 sub-proteomes (Table S1). Proteins identified with only one peptide and in only one out of three experiments, and possibly corresponding to very low abundant proteins, were not analysed further. Finally, we retained 3676 proteins (Table S1). Protein distribution was analysed in the different fractions: 1217 proteins (33.1%) were present in only one fraction and referred to as 'specific proteins', 820 proteins (22.3%) in two fractions, 432 proteins (11.8%) in three fractions, and the rest in more than three fractions (Fig. 3A). An hive plot representation was also used as a rational visualization method for drawing protein distribution (Fig. 3B).[41] A careful analysis of the data showed that abundant proteins, i.e. identified with high weighted spectral count (WSC) values, were distributed in several fractions. The higher the WSC, the more proteins were present in a large number of fractions (Fig. S1).

Properties of native proteins fractionated by anion-exchange chromatography

The behaviour and properties of the 3676 Arabidopsis proteins eluted from the Q-Sepharose column were analysed. The elution profiles of all the identified proteins are displayed in Table S1 and some examples of proteins involved in the antioxidative stress response and metal homeostasis are shown in Fig. S2. As already mentioned the fractionation procedure allowed for a significant enrichment of proteins. The

View Article Online
DOI: 10.1039/D0MT00092B

enrichment factor, calculated on the basis of total proteins in the cell soluble extract and the different fractions, ranged from 7 in F200 to 14 in F100 for specific proteins (eluted in a single fraction). As an example, three ferritin isoforms that were only detected in F200 were enriched 7-fold (Fig. S2). The fractionation procedure also permitted to separate different isoenzymes from the cell soluble protein extract. As an example, the two isoforms of glutathione reductase have been separated from each other (Fig. S2), allowing their individual kinetic and biochemical characterization.

As protein elution during AEC is correlated with the charge of native proteins, we presented the elution profiles according to protein theoretical isoelectric points (pI). Representations of the pI of specific proteins and of the whole set proteins in each fraction are shown in Fig. S3 and theoretical pI values are reported in Table S1. As expected, proteins eluted first from the column have a higher pI than those eluted at higher salt concentrations. For example, the median values of specific proteins identified in F50 and F400 were 8.12 and 5.69, respectively (Fig. S3). In each fraction, several proteins had a pI far from the expected average pI of the fraction. The behaviour of these proteins may be due to the theoretical pI values that are not representative of the distribution of charges at their surface. Another possibility is that some of these proteins are part of protein complexes. For example, several proteins with a high pI were present in F400 (average pI 5.69). Among them, we found the ELF7 protein component of the RNA Polymerase II-associated factor 1 complex (PAF1-C, pI 9.20) and the chloroplast molecular chaperonin CPN60α2 (pI 8.15). Other proteins from these complexes were found in the F400 fraction, as for components of the hexameric PAF1-C complex (VIP3, VIP4 and VIP6/ELF8)[42] or the chloroplast chaperonin (CPN60 α1, β1, β2 and β3).

Survey of the Arabidopsis metalloproteome

To gain insight into the metalloproteome of Arabidopsis cells we analysed the elution profile of metals retained by soluble proteins after AEC. The analysis was done using soluble proteins from control and U-treated cells. First, we found that Mg, K, Ca, Mn, Fe, Cu, and Zn were present in the 10 fractions from Arabidopsis cells treated or not with U (Fig. 4). This result is consistent with the overall abundance of metal-binding proteins in proteomes.[26,27] In contrast, Mo was found almost entirely in F200 (98-99% of the total Mo eluted from the column), with trace amounts in F0, F250, and F300 (Fig. 4). Second, we showed that part of U that was present in the soluble fraction of

Arabidopsis cells (Table 1) was associated with proteins. Indeed, U was detected in several fractions eluted from the Q-Sepharose column. Putative U-binding proteins were mainly present in five fractions (F0, F300, F350, F400 and F1000) and detected in trace amounts in F50 to F250 (Fig. 4). F50 to F1000 were concentrated by ultrafiltration using centrifugal filter devices equipped with a 3 kDa cut-off membrane to verify that U was bound to proteins. For all fractions except F1000, more than 90% of U was recovered in the concentrated protein fractions, thus confirming the interaction of U with proteins. For F1000, up to 80% of U was recovered in the filtrate, suggesting that part of U found in the cell extract was not associated with proteins, or loosely bound to proteins, and eluted from the AEC column with a high salt concentration.

The elution profiles of some metals associated with soluble proteins were modified in cells challenged with U as compared with control cells (Fig. 4). This result suggested that in some cases U might have competed *in vivo* with essentials elements for binding to specific metalloproteins and, in other cases, that U stress triggered perturbations of metal homeostasis leading to an abnormal steady-state level of some metalloproteins.

The elution of Mo as a major peak in F200 (Fig. 4) was surprising since Arabidopsis proteins known to bind the molybdenum cofactor (MoCo) were identified by MS/MS in different fractions eluted from the Q-Sepharose column, with the exception of F200 (Fig. S4). This finding suggested that F200 could contain a previously uncharacterized plant Mo-binding protein. With the aim at identifying this protein by using other chromatographic steps, F200 was concentrated by ultrafiltration using a 3 kDa cut-off membrane. We found that most of Mo was present in the filtrate and, after several cycles of dilution/concentration, F200 contained only residual amounts of Mo. This result suggested that Mo from F200 was not bound tightly to protein(s) but rather present as a free ion or bound to low-molecular weight compounds (e.g. MoCo). To test this hypothesis we analysed the behaviour of free molybdate (MoO_4^{2-}) on the Q-Sepharose column. We found that free molybdate was eluted as a single Mo peak in F200 (not shown). It is therefore possible that Mo detected in F200 from the protein fractionation experiments (Fig. 4) could correspond to a free metal form.

Analysis of post-translational modifications in Arabidopsis sub-proteomes

The AEC fractionation was used to analyse the pattern of post-translationally modified proteins in Arabidopsis cells exposed to U stress. To this aim western-blots were

performed using proteins from Arabidopsis cells challenged or not with uranyl nitrate and with antibodies recognizing trimethylated lysine (Lys) (Fig. 5B) or asymmetrically dimethylated arginine (Arg) (Fig. 5C). Post-translational methylation of Lys and Arg residues in proteins have essential regulatory functions in all cellular processes and are predicted to play a crucial role in enabling plants to cope with biotic and abiotic stresses.[43-45] In support of this assumption, we have recently shown that protein Lys methylation contributes in modulating the response of Arabidopsis plants to a stress induced by cadmium.[46] Immunoblots with total soluble proteins revealed a few methylated polypeptides whereas those realized with the fractions separated by AEC showed additional methylated proteins. We further analysed the dimethylated Arg signal that was detected in a 15-20 kDa polypeptide in F100 and that was more strongly immuno-labelled in U-stressed than in control cells (Fig. 5D). With the aim at identifying this polypeptide, F100 fractions from untreated and U-treated cells were resolved by SDS-PAGE, bands at 15-20 kDa were excised from the gel, digested with trypsin, and peptides were analysed by LC-MS/MS using a Q-Exactive Plus Orbitrap mass spectrometer. To identify methyl peptides, MS/MS spectra were searched for mass shifts corresponding to mono and dimethylation of Arg residues but also mono, di and trimethylation of Lys residues in order to minimize assignation errors for peptides bearing both amino acids (Table S2).[47] The analysis identified ten dimethyl Arg and 30 monomethyl Arg peptides belonging to 33 distinct proteins, of which eight had the expected size (<20 kDa). A single protein was found dimethylated at the level of Arg residues in much higher proportions in F100 from U-treated cells (F100_U50) compared with F100 from untreated control cells (F100_U0), which matches well with the western blot profile (Fig. 5D; Table S2). Indeed, the 40S ribosomal protein S10-3 (RPS10C) was dimethylated at the level of Arg159 and Arg163 residues in F100_U50. These residues were also detected in their unmethylated forms, and in equivalent proportions, in this fraction. In contrast, Arg159 and Arg163 were detected exclusively in their unmethylated state in F100_U0. A second protein, the actin-depolymerizing factor 1 (ADF1), was found monomethylated at the level of Arg66 in F100_U50 at higher proportions than in F100_U0. However, since the asymmetric dimethyl Arg monoclonal antibody used in our experiments is highly specific and in particular does not cross-react with monomethyl Arg residues,[48-50] the hypothesis according to which ADF1 could be the labelled band detected by western blot in F100_U50 could be ruled out. Taken together, these data indicated that the steady-state level and/or the

methylation stoichiometry of Arg159 and Arg163 in RPS10C are increased in Arabidopsis cells challenged with U.

Conclusion

In the present work, we have developed an ionomic, metalloproteomic, and biochemical toolbox to analyse the consequences of uranyl stress on the proteome of Arabidopsis cells. First, the ionomic analysis of Arabidopsis cells challenged with U showed that the homeostasis of K, Mg, Fe, Mn and Zn was significantly affected, with a reduction in pool size measured in whole cells, and/or protoplasts, and/or cell soluble fractions (Table 1). These results are consistent with the perturbations of mineral nutrition observed in the roots of uranyl-treated Arabidopsis plants[14] and they provide further indications about which cellular pools of essential elements are affected by U stress. Ionomic data also showed that the cell wall plays a major role in the binding of U and is probably an important defence mechanism for plants to limit the accumulation of the radionuclide in the protoplast and cytoplasm, as evidenced for other toxic elements.[51,52] The accumulation of up to 65% of U in the cell wall of Arabidopsis cultured cells (Fig. 1) is consistent with previous data showing that U-treated plants display important U precipitates in the cell wall of root cells.[9,10,53] Cell walls are primarily composed of polysaccharides (cellulose, pectins, hemicelluloses) and (glyco)proteins that provide negatively charged groups on which the uranyl ion may bind. For example, carboxyl groups from low methyl-esterified pectins,[51] together with phosphate,[10] confer to the cell wall a high cation exchange capacity. Our ionomic data also confirmed previous studies indicating that the plant cell wall acts either as a reservoir of some essential elements, which can possibly be (re)mobilized in response to a nutritional deficiency (e.g. Fe),[54] or as a pool of metabolically-active bound-metals, such as Cu that is bound to proteins involved in cell wall loosening/strengthening mechanisms.[55]

Second, high-resolution fractionation of Arabidopsis cell soluble proteins into 10 subproteomes by AEC has proven to be a very efficient method for top-down proteomics, invaluable for reducing sample complexity and improving proteome coverage through enrichment of low-abundant proteins. The protein enrichment factors obtained with this procedure (up to 14-fold) are similar to those obtained by purification of plant mitochondria and higher than those for purified chloroplasts.[56,57] Our data provide the plant biologist community with a useful resource concerning the behaviour

and the pre-purification of 3676 protein isoforms (and up to 6603 entries if all proteins are included) with the advantage of being directly recovered in solution for further purification and/or biochemical analysis.

Third, despite the low amount of U that reached the cell soluble fraction (less than 2% in our experimental conditions), we showed that several pools of Arabidopsis proteins are able to bind the radionuclide tightly. Uranium has been found in several fractions from the AEC but the complexity of these protein samples is still too high to identify Arabidopsis uranyl-binding proteins. However, U has been shown to bind to Ca-binding proteins (e.g. calmodulin) or Fe-binding proteins (e.g. ferritin) in eukaryotes or bacterial cells.[30,58] Fractions containing homologs of these proteins in Arabidopsis contain varying amounts of U (Fig. 4), suggesting that calmodulin isoforms (CAM1 and CAM7 eluted in F300 to F1000) or ferritin (eluted in F200) could also be plant uranyl-binding proteins. However, at this stage of the purification process, the U/Ca or U/Fe ratio is too low to conclude about the nature of U-protein complexes. Further purification steps should be used following AEC fractionation to identify authentic plant proteins able to bind uranyl *in vivo*.

Last, the fractionation procedure allowed us to analyse the Lys and Arg methylation status of proteins from Arabidopsis cells challenged with U. We showed that U induced a modification of the methylation pattern of some proteins, as previously observed in Arabidopsis plants treated with cadmium.[46] Also, MS/MS analysis identified that the 40S ribosomal protein RPS10C was dimethylated at Arg159 and Arg163 following U stress. This is the first evidence of methylation of this protein in plants despite the comprehensive analysis of post-translational modifications of the 80S cytosolic ribosome.[59] Interestingly, methylation of the human ortholog RPS10 at equivalent Arg positions (Arg158 and Arg160) plays a role in the proper assembly of ribosomes, protein synthesis, and optimal cell proliferation.[60] The human protein Arg methyltransferase 5 (PRMT5) is responsible for the methylation of RPS10. The homolog of PRMT5 in Arabidopsis, AtPRMT5, plays a role in the methylation of histone H4R3 and is involved in the control of flowering time.[61] RPS10C could be an alternative substrate of AtPRMT5 in Arabidopsis and it is possible that this protein Arg methyltransferase plays a role in the regulation of plant response to U stress. This finding, together with recent evidence that protein Lys methylation modulates the response of Arabidopsis to cadmium,[46] suggests that post-translational modifications are essential mechanisms for plants to cope with metals. The present toolbox is a

starting platform to further characterize the role of these modifications in metal stress response in Arabidopsis.

Bibliographic references

1. H. Vandenhove, European sites contaminated by residues from the ore-extracting and-processing industries, *International Congress Series*, 2002, **1225**, 307-315.
2. M. Anke, O. Seeber, R. Mueller, U. Schaefer and J. Zerull, Uranium transfer in the food chain from soil to plants, animals and man, *Chemie Der Erde-Geochemistry*, 2009, **69**, 75-90.
3. E. Schnug and B. G. Lottermoser, Fertilizer-Derived Uranium and its Threat to Human Health, *Environmental Science & Technology*, 2013, **47**, 2433-2434.
4. N. Gao, Z. Huang, H. Liu, J. Hou and X. Liu, Advances on the toxicity of uranium to different organisms, *Chemosphere*, 2019, **237**.
5. R. G. Pearson, HARD AND SOFT ACIDS AND BASES, *J. Am. Chem. Soc.*, 1963, **85**, 3533-&.
6. A. Garai and P. Delangle, Recent advances in uranyl binding in proteins thanks to biomimetic peptides, *J. Inorg. Biochem.*, 2020, **203**, 110936-110936.
7. S. D. Ebbs, D. J. Brady and L. V. Kochian, Role of uranium speciation in the uptake and translocation of uranium by plants, *J. Exp. Bot.*, 1998, **49**, 1183-1190.
8. N. Vanhoudt, H. Vandenhove, K. Smeets, T. Remans, M. Van Hees, J. Wannijn, J. Vangronsveld and A. Cuypers, Effects of uranium and phosphate concentrations on oxidative stress related responses induced in Arabidopsis thaliana, *Plant Physiol. Biochem.*, 2008, **46**, 987-996.
9. J. Misson, P. Henner, M. Morello, M. Floriani, T. D. Wu, J. L. Guerquin-Kern and L. Fevrier, Use of phosphate to avoid uranium toxicity in Arabidopsis thaliana leads to alterations of morphological and physiological responses regulated by phosphate availability, *Environ. Exp. Bot.*, 2009, **67**, 353-362.
10. J. Laurette, C. Larue, I. Llorens, D. Jaillard, P. H. Jouneau, J. Bourguignon and M. Carrière, Speciation of uranium in plants upon root accumulation and root-to-shoot translocation: A XAS and TEM study, *Environ. Exp. Bot.*, 2012, **77**, 87– 95.
11. J. Laurette, C. Larue, C. Mariet, F. Brisset, H. Khodjad, J. Bourguignon and M. Carrière, Influence of uranium speciation on its accumulation and translocation in three plant species: Oilseed rape, sunflower and wheat, *Environ. Exp. Bot.*, 2012, **77**, 96-107.
12. N. Vanhoudt, A. Cuypers, N. Horemans, T. Remans, K. Opdenakker, K. Smeets, D. M. Bello, M. Havaux, J. Wannijn, M. Van Hees, J. Vangronsveld and H. Vandenhove, Unraveling uranium induced oxidative stress related responses in *Arabidopsis thaliana* seedlings. Part II: responses in the leaves and general conclusions, *J. Environ. Radioactiv.*, 2011, **102**, 638-645.
13. N. Vanhoudt, N. Horemans, G. Biermans, E. Saenen, J. Wannijn, R. Nauts, M. Van Hees and H. Vandenhove, Uranium affects photosynthetic parameters in *Arabidopsis thaliana*, *Environ. Exp. Bot.*, 2014, **97**, 22-29.
14. N. Vanhoudt, H. Vandenhove, N. Horemans, D. M. Bello, M. Van Hees, J. Wannijn, R. Carleer, J. Vangronsveld and A. Cuypers, Uranium induced effects on development and mineral nutrition of *Arabidopsis thaliana*, *J. Plant Nutr.*, 2011, **34**, 1940-1956.
15. N. Vanhoudt, H. Vandenhove, N. Horemans, T. Remans, K. Opdenakker, K. Smeets, D. M. Bello, J. Wannijn, M. Van Hees, J. Vangronsveld and A. Cuypers, Unraveling uranium induced oxidative stress related responses in *Arabidopsis thaliana* seedlings. Part I: responses in the roots, *J. Environ. Radioactiv.*, 2011, **102**, 630-637.
16. I. Aranjuelo, F. Doustaly, J. Cela, R. Porcel, M. Mueller, R. Aroca, S. Munne-Bosch and J. Bourguignon, Glutathione and transpiration as key factors conditioning oxidative stress in Arabidopsis thaliana exposed to uranium, *Planta*, 2014, **239**, 817-830.

17. E. Saenen, N. Horemans, N. Vanhoudt, H. Varidenhove, G. Biermans, M. Van Hees, J. Wannijn, J. Vangronsveld and A. Cuypers, The pH strongly influences the uranium-induced effects on the photosynthetic apparatus of Arabidopsis thaliana plants, *Plant Physiol. Biochem.*, 2014, **82**, 254-261.
18. E. Saenen, N. Horemans, N. Vanhoudt, H. Vandenhove, G. Biermans, M. Van Hees, J. Wannijn, J. Vangronsveld and A. Cuypers, Induction of Oxidative Stress and Antioxidative Mechanisms in Arabidopsis thaliana after Uranium Exposure at pH 7.5, *Int. J. Mol. Sci.*, 2015, **16**, 12405-12423.
19. N. B. C. Serre, C. Alban, J. Bourguignon and S. Ravanel, Uncovering the physiological and cellular effects of uranium on the root system of Arabidopsis thaliana, *Environ. Exp. Bot.*, 2019, **157**, 121-130.
20. R. Tewari, N. Horemans, R. Nauts, J. Wannijn, M. Van Hees and H. Vandenhove, Uranium exposure induces nitric oxide and hydrogen peroxide generation in Arabidopsis thaliana, *Environ. Exp. Bot.*, 2015, **120**, 55-64.
21. F. Doustaly, C. Combes, J. Fiévet, S. Berthet, V. Hugouvieux, O. Bastien, I. Aranjuelo, N. Leonhardt, C. Rivasseau, M. Carrière, A. Vavasseur, J. P. Renou, Y. Vandenbrouck and J. Bourguignon, Uranium perturbs signaling and iron uptake response in Arabidopsis thaliana roots, *Metallomics*, 2014, **6**, 809--821.
22. S. Berthet, F. Villiers, C. Alban, N. B. C. Serre, J. Martin-Laffon, S. Figuet, A. M. Boisson, R. Bligny, M. Kuntz, G. Finazzi, S. Ravanel and J. Bourguignon, Arabidopsis thaliana plants challenged with uranium reveal new insights into iron and phosphate homeostasis, *New Phytol.*, 2018, **217**, 657-670.
23. J.-L. Lai, Z.-W. Liu and X.-G. Luo, A metabolomic, transcriptomic profiling, and mineral nutrient metabolism study of the phytotoxicity mechanism of uranium, *J. Hazard. Mat.*, 2020, **386**, 121437.
24. J. P. Barnett, D. J. Scanlan and C. A. Blindauer, Protein fractionation and detection for metalloproteomics: challenges and approaches, *Analytical and Bioanalytical Chemistry*, 2012, **402**, 3311-3322.
25. A. Hagège, T. N. S. Huynh and M. Hébrant, Separative techniques for metalloproteomics require balance betweenseparation and perturbation, *Trends Anal. Chem.*, 2015, **64**, 64-74.
26. W. Shi and M. R. Chance, Metalloproteomics: forward and reverse approaches in metalloprotein structural and functional characterization, *Curr. Opin. Chem. Biol.*, 2011, **15**, 144-148.
27. S. M. Yannone, S. Hartung, A. L. Menon, M. W. W. Adams and J. A. Tainer, Metals in biology: defining metalloproteomes, *Curr. Opin. Biotechnol.*, 2012, **23**, 89-95.
28. C. C. S. Kung, W. N. Huang, Y. C. Huang and K. C. Yeh, Proteomic survey of copper-binding proteins in Arabidopsis roots by immobilized metal affinity chromatography and mass spectrometry, *Proteomics*, 2006, **6**, 2746-2758.
29. Y.-F. Tan, N. O'Toole, N. L. Taylor and A. H. Millar, Divalent Metal Ions in Plant Mitochondria and Their Role in Interactions with Proteins and Oxidative Stress-Induced Damage to Respiratory Function, *Plant Physiol.*, 2010, **152**, 747-761.
30. A. Cvetkovic, A. L. Menon, M. P. Thorgersen, J. W. Scott, F. L. Poole, F. E. Jenney, W. A. Lancaster, J. L. Praissman, S. Shanmukh, B. J. Vaccaro, S. A. Trauger, E. Kalisiak, J. V. Apon, G. Siuzdak, S. M. Yannone, J. A. Tainer and M. W. W. Adams, Microbial metalloproteomes are largely uncharacterized, *Nature*, 2010, **466**, 779-U718.
31. J. P. Barnett, D. J. Scanlan and C. A. Blindauer, Identification of major zinc-binding proteins from a marine cyanobacterium: insight into metal uptake in oligotrophic environments, *Metallomics*, 2014, **6**, 1254-1268.
32. D. J. Hare, A. Grubman, T. M. Ryan, A. Lothian, J. R. Liddell, R. Grimm, T. Matsuda, P. A. Doble, R. A. Cherny, A. I. Bush, A. R. White, C. L. Masters and B. R. Roberts, Profiling the iron, copper and zinc content in primary neuron and astrocyte cultures by rapid online

quantitative size exclusion chromatography-inductively coupled plasma-mass spectrometry, *Metallomics*, 2013, **5**, 1656-1662.

33. M. Xu, S. Frelon, O. Simon, R. Lobinski and S. Mounicou, Development of a non-denaturing 2D gel electrophoresis protocol for screening in vivo uranium-protein targets in Procambarus clarkii with laser ablation ICP MS followed by protein identification by HPLC-Orbitrap MS, *Talanta*, 2014, **128**, 187-195.
34. Y. Eb-Levadoux, S. Frelon, O. Simon, C. Arnaudguilhem, R. Lobinski and S. Mounicou, In vivo identification of potential uranium protein targets in zebrafish ovaries after chronic waterborne exposure, *Metallomics*, 2017, **9**, 525-534.
35. C. Vidaud, M. Robert, E. Paredes, R. Ortega, E. Avazeri, L. Jing, J.-M. Guigonis, C. Bresson and V. Malard, Deciphering the uranium target proteins in human dopaminergic SH-SY5Y cells, *Arch. Toxicol.*, 2019, **93**, 2141-2154.
36. M. M. Bradford, RAPID AND SENSITIVE METHOD FOR QUANTITATION OF MICROGRAM QUANTITIES OF PROTEIN UTILIZING PRINCIPLE OF PROTEIN-DYE BINDING, *Anal. Biochem.*, 1976, **72**, 248-254.
37. V. Dupierris, C. Masselon, M. Court, S. Kieffer-Jaquinod and C. Bruley, A toolbox for validation of mass spectrometry peptides identification and generation of database: IRMa, *Bioinformatics*, 2009, **25**, 1980-1981.
38. A.-M. Hesse, V. Dupierris, C. Adam, M. Court, D. Barthe, A. Emadali, C. Masselon, M. Ferro and C. Bruley, hEIDI: An Intuitive Application Tool To Organize and Treat Large-Scale Proteomics Data, *Journal of Proteome Research*, 2016, **15**, 3896-3903.
39. S. Tyanova, T. Temu and J. Cox, The MaxQuant computational platform for mass spectrometry-based shotgun proteomics, *Nature Protocols*, 2016, **11**, 2301-2319.
40. H. Canut, C. Albenne and E. Jamet, Isolation of the Cell Wall, *Methods in molecular biology (Clifton, N.J.)*, 2017, **1511**, 171-185.
41. M. Krzywinski, I. Birol, S. J. M. Jones and M. A. Marra, Hive plots-rational approach to visualizing networks, *Briefings in Bioinformatics*, 2012, **13**, 627-644.
42. W. Antosz, A. Pfab, H. F. Ehrnsberger, P. Holzinger, K. Koellen, S. A. Mortensen, A. Bruckmann, T. Schubert, G. Laengst, J. Griesenbeck, V. Schubert, M. Grasser and K. D. Grasser, The Composition of the Arabidopsis RNA Polymerase II Transcript Elongation Complex Reveals the Interplay between Elongation and mRNA Processing Factors, *Plant Cell*, 2017, **29**, 854-870.
43. N. B. C. Serre, C. Alban, J. Bourguignon and S. Ravanel, An outlook on lysine methylation of non-histone proteins in plants, *J. Exp. Bot.*, 2018, **69**, 4569-4581.
44. J. Dahan, E. Koen, D. A., O. Lamotte and S. Bourque, *Abiotic Stress Response in Plants: Physiological, Biochemical and Genetic Perspectives*, 2011.
45. K. Kosova, P. Vitamvas, I. T. Prasil and J. Renaut, Plant proteome changes under abiotic stress - Contribution of proteomics studies to understanding plant stress response, *J. Proteomics*, 2011, **74**, 1301-1322.
46. N. B. C. Serre, M. Sarthou, O. Gigarel, S. Figuet, M. Corso, J. Choulet, V. Rofidal, C. Alban, V. Santoni, J. Bourguignon, N. Verbruggen and S. Ravanel, Protein lysine methylation contributes to modulating the response of sensitive and tolerant Arabidopsis species to cadmium stress, *Plant Cell Environ.*, 2020, DOI: 10.1111/pce.13692.
47. C. Alban, M. Tardif, M. Mininno, S. Brugiere, A. Gilgen, S. Ma, M. Mazzoleni, O. Gigarel, J. Martin-Laffon, M. Ferro and S. Ravanel, Uncovering the Protein Lysine and Arginine Methylation Network in Arabidopsis Chloroplasts, *Plos One*, 2014, **9**, 13.
48. S. Dhar, V. Vemulapalli, A. N. Patananan, G. L. Huang, A. Di Lorenzo, S. Richard, M. J. Comb, A. Guo, S. G. Clarke and M. T. Bedford, Loss of the major Type I arginine methyltransferase PRMT1 causes substrate scavenging by other PRMTs, *Sci Rep*, 2013, **3**, 1311.
49. M. Bremang, A. Cuomo, A. M. Agresta, M. Stugiewicz, V. Spadotto and T. Bonaldi, Mass spectrometry-based identification and characterisation of lysine and arginine methylation in the human proteome, *Mol Biosyst*, 2013, **9**, 2231-2247.

50. A. L. Guo, H. B. Gu, J. Zhou, D. Mulhern, Y. Wang, K. A. Lee, V. Yang, M. Aguiar, J. Kornhauser, X. Y. Jia, J. M. Ren, S. A. Beausoleil, J. C. Silva, V. Vemulapalli, M. T. Bedford and M. J. Comb, Immunoaffinity Enrichment and Mass Spectrometry Analysis of Protein Methylation, *Molecular & Cellular Proteomics*, 2014, **13**, 372-387.
51. M. Krzeslowska, The cell wall in plant cell response to trace metals: polysaccharide remodeling and its role in defense strategy, *Acta Physiol. Plant.*, 2011, **33**, 35-51.
52. H. Le Gall, F. Philippe, J.-M. Domon, F. Gillet, J. Pelloux and C. Rayon, Cell Wall Metabolism in Response to Abiotic Stress, *Plants (Basel, Switzerland)*, 2015, **4**, 112-166.
53. E. El Hayek, A. J. Brearley, T. Howard, P. Hudson, C. Torres, M. N. Spilde, S. Cabaniss, A.-M. S. Ali and J. M. Cerrato, Calcium in Carbonate Water Facilitates the Transport of U(VI) in Brassica juncea Roots and Enables Root-to-Shoot Translocation, *Acs Earth and Space Chemistry*, 2019, **3**, 2190-2196.
54. C. Curie and S. Mari, New routes for plant iron mining, *New Phytol.*, 2017, **214**, 521-525.
55. B. Printz, S. Lutts, J.-F. Hausman and K. Sergeants, Copper Trafficking in Plants and Its Implication on Cell Wall Dynamics, *Front. Plant Sci.*, 2016, **7**.
56. J. Puyaubert, L. Denis and C. Alban, Dual targeting of Arabidopsis holocarboxylase synthetase1: A small upstream open reading frame regulates translation initiation and protein targeting, *Plant Physiol.*, 2008, **146**, 478-491.
57. S. Jabrin, S. Ravanel, B. Gambonnet, R. Douce and F. Rebeille, One-carbon metabolism in plants. Regulation of tetrahydrofolate synthesis during germination and seedling development, *Plant Physiol.*, 2003, **131**, 1431-1439.
58. L. Le Clainche and C. Vita, Selective binding of uranyl cation by a novel calmodulin peptide, *Environmental Chemistry Letters*, 2006, **4**, 45-49.
59. A. J. Carroll, J. L. Heazlewood, J. Ito and A. H. Millar, Analysis of the Arabidopsis cytosolic ribosome proteome provides detailed insights into its components and their post-translational modification, *Molecular & Cellular Proteomics*, 2008, **7**, 347-369.
60. J. Q. Ren, Y. Q. Wang, Y. H. Liang, Y. Q. Zhang, S. L. Bao and Z. H. Xu, Methylation of Ribosomal Protein S10 by Protein-arginine Methyltransferase 5 Regulates Ribosome Biogenesis, *J. Biol. Chem.*, 2010, **285**, 12695-12705.
61. X. Wang, Y. Zhang, Q. B. Ma, Z. L. Zhang, Y. B. Xue, S. L. Bao and K. Chong, SKB1-mediated symmetric dimethylation of histone H4R3 controls flowering time in Arabidopsis, *EMBO J.*, 2007, **26**, 1934-1941.
62. B. A. Hanson, HiveR: 2D and 3D Hive Plots for R, 2011, **R package version 0.1-3**.
63. F. Bittner, Molybdenum metabolism in plants and crosstalk to iron, *Front. Plant Sci.*, 2014, **5**.

Figure legends

Table 1: Ionomic analysis of Arabidopsis cells challenged with U.

Exponentially-growing Arabidopsis cells were transferred into MS medium with low Pi content in the absence (U0) or presence of 50 µM uranyl nitrate (U50). Cells were harvested after 24 h of incubation and used to prepare protoplasts and soluble fractions. Cell samples were digested in nitric oxide and analysed by ICP-MS. Elemental content is expressed in µg element.mg^{-1} protein. Means ± SD are shown (n=6 independent cultures for U0 and U50). Statistical significance for the comparison U50 to U0 was determined using a non-parametric Dunnett's test, with $p < 0.05$ (*), and $p < 0.01$ (**).

Figure 1: Distribution of elements between the cell wall and the protoplast in Arabidopsis cells challenged with U.

The elemental composition of Arabidopsis cells and protoplasts challenged (U50) or not (U0) with uranyl nitrate is given in Table 1. These data have allowed to calculate the distribution of elements between the cell wall (■) and the protoplast (□), assuming that cell wall proteins account for 0.5 to 6% of total cellular proteins.[40] Means ± SD are shown (n=6 independent cultures for U0 and U50).

Figure 2: Fractionation of Arabidopsis soluble proteins by anion-exchange chromatography.

A- Distribution of proteins in the 10 fractions from the AEC column. Soluble proteins from Arabidopsis cells (about 40 mg protein) were fractionated onto a Q-Sepharose High Performance column (1.6 x 5 cm) using a step-gradient of NaCl (0 to 1 M) in 10 mM Tris-HCl, pH 7.5, 1 mM dithiothreitol. Boxplots show the distribution of proteins for 4 independent analyses. B- SDS-PAGE analysis of proteins from the 10 fractions. Each gel shows protein profiles of one of the four independent fractionation experiments. M, molecular mass markers in kDa.

Figure 3: Distribution of proteins identified by MS/MS in fractions from anion-exchange chromatography.

View Article Online
DOI: 10.1039/D0MT00092B

A- Resolution of the AEC column as estimated by the number of fractions in which the proteins identified by MS/MS are distributed. More than 55% of the identified proteins are present in one or two fractions eluted from the Q-Sepharose column. B- Hive plot representation of proteins distribution in fractions from the AEC column. The distribution of proteins in the different fractions is represented as a network and was created using the HiveR R package.[62] Linear axes represent the fractions (F0 to F1000); their length is proportional to the number of identified proteins in the fraction and their thickness is proportional to the numbers of proteins specifically present in the fraction. The curved lines connecting two axes symbolize the presence of the same protein in both fractions.

Figure 4: Elemental profiling in fractions from anion-exchange chromatography. Soluble proteins (40 mg) from Arabidopsis cells grown for 24 h in the absence (U0) or presence of 50 µM uranyl nitrate (U50) were resolved by AEC on a Q-Sepharose column. Metals were extracted from proteins in 10% (v/v) nitric acid and analysed by ICP-MS. The elution profiles of each element in control (□) and U-challenged cells (■) are shown. Means ± SD for n=3 elemental analyses of representative AEC experiments.

Figure 5: Immunodetection of lysine and arginine methylated proteins in Arabidopsis cells challenged with U.

A- SDS-PAGE analysis of soluble proteins extracted from Arabidopsis cells grown for 24 h in the absence (U0) or presence of 50 µM uranyl nitrate (U50) and resolved by AEC on a Q-Sepharose column. Gel image for U0 is similar to the one from Fig. 2B, upper-right panel. B- Immunodetection of trimethyl-Lys in AEC fractions. C- Immunodetection of asymmetric dimethyl-Arg in AEC fractions. D- Closer views of SDS-PAGE and immunoblot for the fraction eluted at 100 mM NaCl. The band excised from the gel for MS/MS identification of Arg-methylated proteins is outlined in red. M, molecular mass markers, in kDa; T, total soluble extract; F0 to F1000, fractions eluted from the Q-Sepharose column from 0 (run-off) to 1000 mM NaCl.

Figure S1: Influence of protein abundance on protein distribution in anion-exchange chromatography fractions.

The abundance of proteins identified by MS/MS was calculated using weighted spectral count (WSC) values. The higher the WSC, the more proteins were present in a large number of fractions.

Figure S2: Elution profiles of metal- and stress-related proteins fractionated by anion-exchange chromatography. Some proteins involved in oxidative stress response and metal homeostasis were retrieved from MS/MS data and their elution profiles on Q-Sepharose were produced using WSC values.

Figure S3: Influence of isoelectric point on protein distribution in anion-exchange chromatography fractions.
Theoretical isoelectric points (pI) of full-length proteins were obtained from the TAIR database. A- Distribution of pI for specific proteins (eluted in a single fraction). B- Distribution of pI for all proteins. The average pI value for each fraction is indicated below boxplots.

Figure S4: Elution profiles of MoCo containing proteins fractionated by anion-exchange chromatography. Molybdo-enzymes[63] were retrieved from MS/MS data and their elution profiles on Q-Sepharose were produced using WSC values.

Table S1: Proteins identified by LC MS/MS in Arabidopsis cell soluble fractions separated by Q-Sepharose chromatography.

Table S2: Proteins identified by LC MS/MS in F100 from U-stressed and control Arabidopsis cells.

Table 1: Ionomic analysis of Arabidopsis cells challenged with U.

Exponentially-growing Arabidopsis cells were transferred into MS medium with low Pi content in the absence (U0) or presence of 50 µM uranyl nitrate (U50). Cells were harvested after 24 h of incubation and used to prepare protoplasts and soluble fractions. Cell samples were digested in nitric oxide and analysed by ICP-MS. Elemental content is expressed in µg element.mg^{-1} protein. Means ± SD are shown (n=6 independent cultures for U0 and U50). Statistical significance for the comparison U50 to U0 was determined using a non-parametric Dunnett's test, with $p < 0.05$ (*), and $p < 0.01$ (**).

	Cells		Protoplasts		Soluble fractions	
	U0	U50	U0	U50	U0	U50
Mg	24.7 ± 1.6	24.0 ± 2.7	9.8 ± 1.0	8.4 ± 0.6 **	13.4 ± 1.5	11.2 ± 1.4 *
K	513.6 ± 37.4	453.2 ± 25.6 *	84.6 ± 7.7	63.3 ± 12.1 **	128.1 ± 23.8	101.4 ± 30.5
Ca	15.7 ± 1.6	17.6 ± 2.6	13.5 ± 3.8	16.1 ± 3.7	10.8 ± 1.3	10.9 ± 1.8
Mn	0.87 ± 0.24	0.97 ± 0.24	0.27 ± 0.11	0.30 ± 0.09	0.18 ± 0.02	0.14 ± 0.02 *
Fe	1.96 ± 0.25	1.43 ± 0.34 *	0.62 ± 0.25	0.58 ± 0.16	0.31 ± 0.03	0.26 ± 0.03
Cu	0.023 ± 0.004	0.020 ± 0.002	0.019 ± 0.005	0.019 ± 0.009	0.013 ± 0.002	0.013 ± 0.004
Zn	1.51 ± 0.43	1.64 ± 0.39	0.54 ± 0.20	0.55 ± 0.16	0.46 ± 0.07	0.37 ± 0.03 **
Mo	0.106 ± 0.015	0.114 ± 0.021	0.037 ± 0.004	0.031 ± 0.006	0.055 ± 0.008	0.060 ± 0.010
U	0.00 ± 0.00	7.15 ± 2.07 **	0.00 ± 0.00	2.67 ± 0.48 **	0.00 ± 0.00	0.10 ± 0.05 **

Figure 1

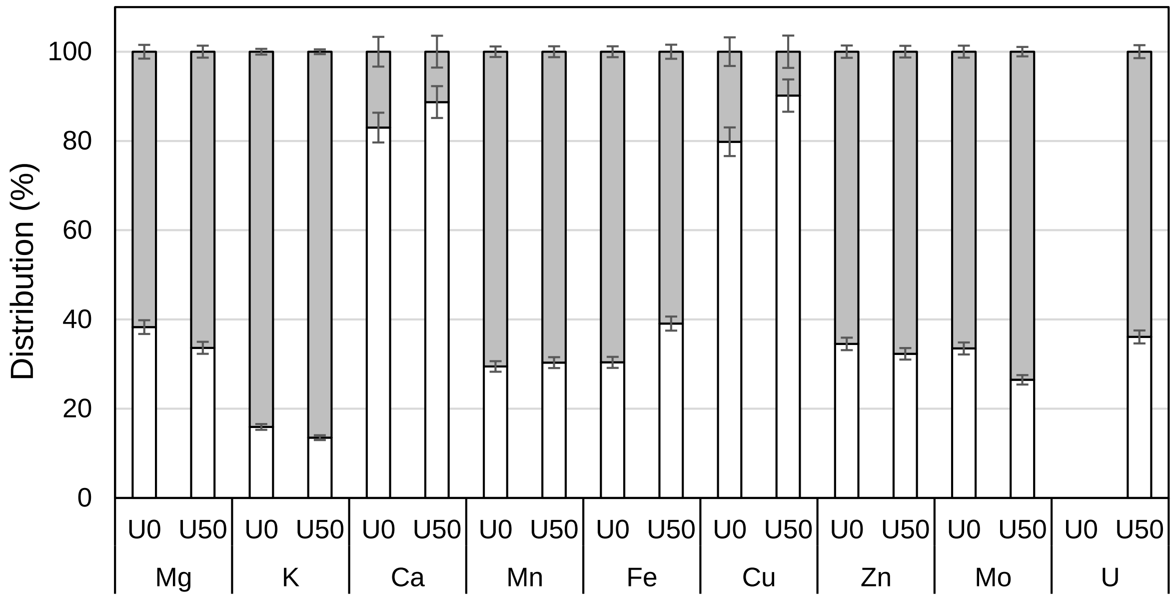

Figure 1: Distribution of elements between the cell wall and the protoplast in Arabidopsis cells challenged with U.
The elemental composition of Arabidopsis cells and protoplasts challenged (U50) or not (U0) with uranyl nitrate is given in Table 1. These data have allowed to calculate the distribution of elements between the cell wall (■) and the protoplast (□), assuming that cell wall proteins account for 0.5 to 6% of total cellular proteins.[40] Means ± SD are shown (n=6 independent cultures for U0 and U50).

Figure 2

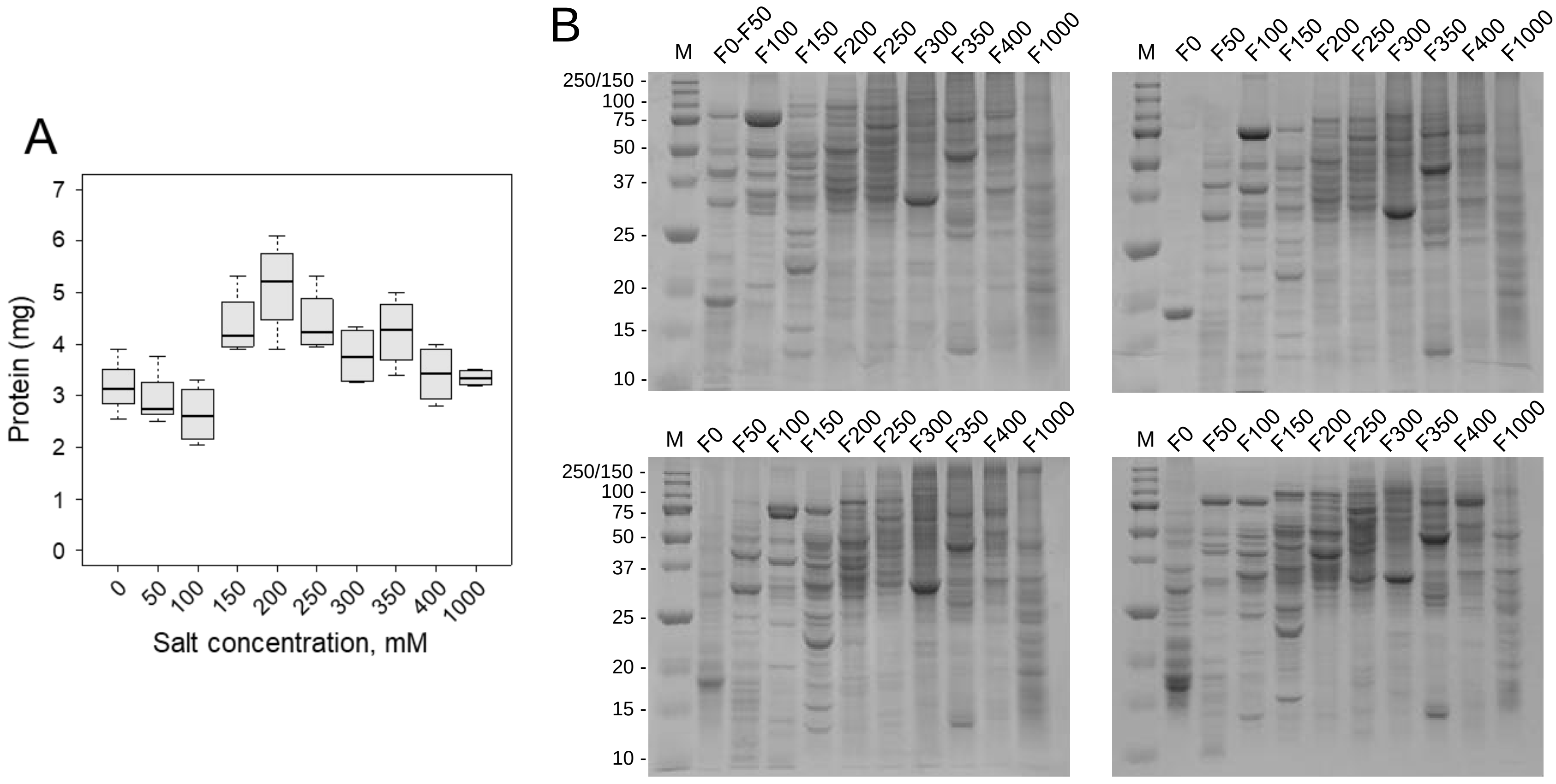

Figure 2: Fractionation of Arabidopsis soluble proteins by anion-exchange chromatography.
A- Distribution of proteins in the 10 fractions from the AEC column. Soluble proteins from Arabidopsis cells (about 40 mg protein) were fractionated onto a Q-Sepharose High Performance column (1.6 x 5 cm) using a step-gradient of NaCl (0 to 1 M) in 10 mM Tris-HCl, pH 7.5, 1 mM dithiothreitol. Boxplots show the distribution of proteins for 4 independent analyses. B- SDS-PAGE analysis of proteins from the 10 fractions. Each gel shows protein profiles of one of the four independent fractionation experiments. M, molecular mass markers in kDa.

Figure 3

A

Number of fractions	Number of proteins
1	1217
2	820
3	432
4	330
5	265
6	216
7	157
8	94
9	74
10	71
Total	**3676**

B

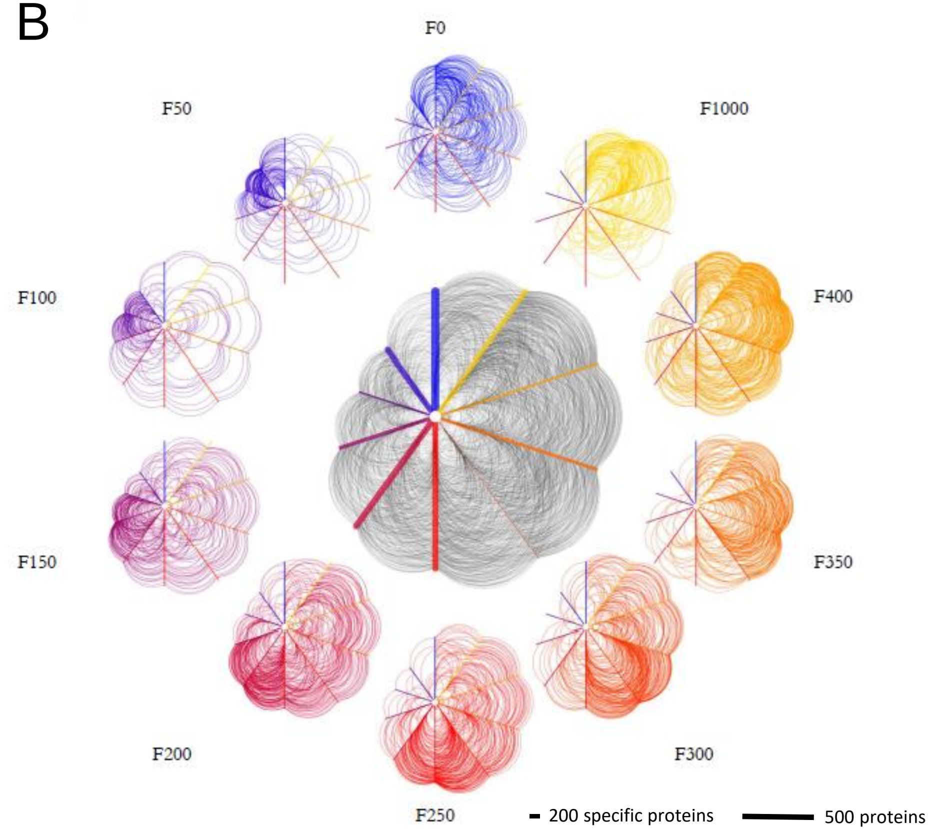

Figure 3: Distribution of proteins identified by MS/MS in fractions from anion-exchange chromatography.
A- Resolution of the AEC column as estimated by the number of fractions in which the proteins identified by MS/MS are distributed. More than 55% of the identified proteins are present in one or two fractions eluted from the Q-Sepharose column. B- Hive plot representation of proteins distribution in fractions from the AEC column. The distribution of proteins in the different fractions is represented as a network and was created using the HiveR R package.[62] Linear axes represent the fractions (F0 to F1000); their length is proportional to the number of identified proteins in the fraction and their thickness is proportional to the numbers of proteins specifically present in the fraction. The curved lines connecting two axes symbolize the presence of the same protein in both fractions.

Figure 4

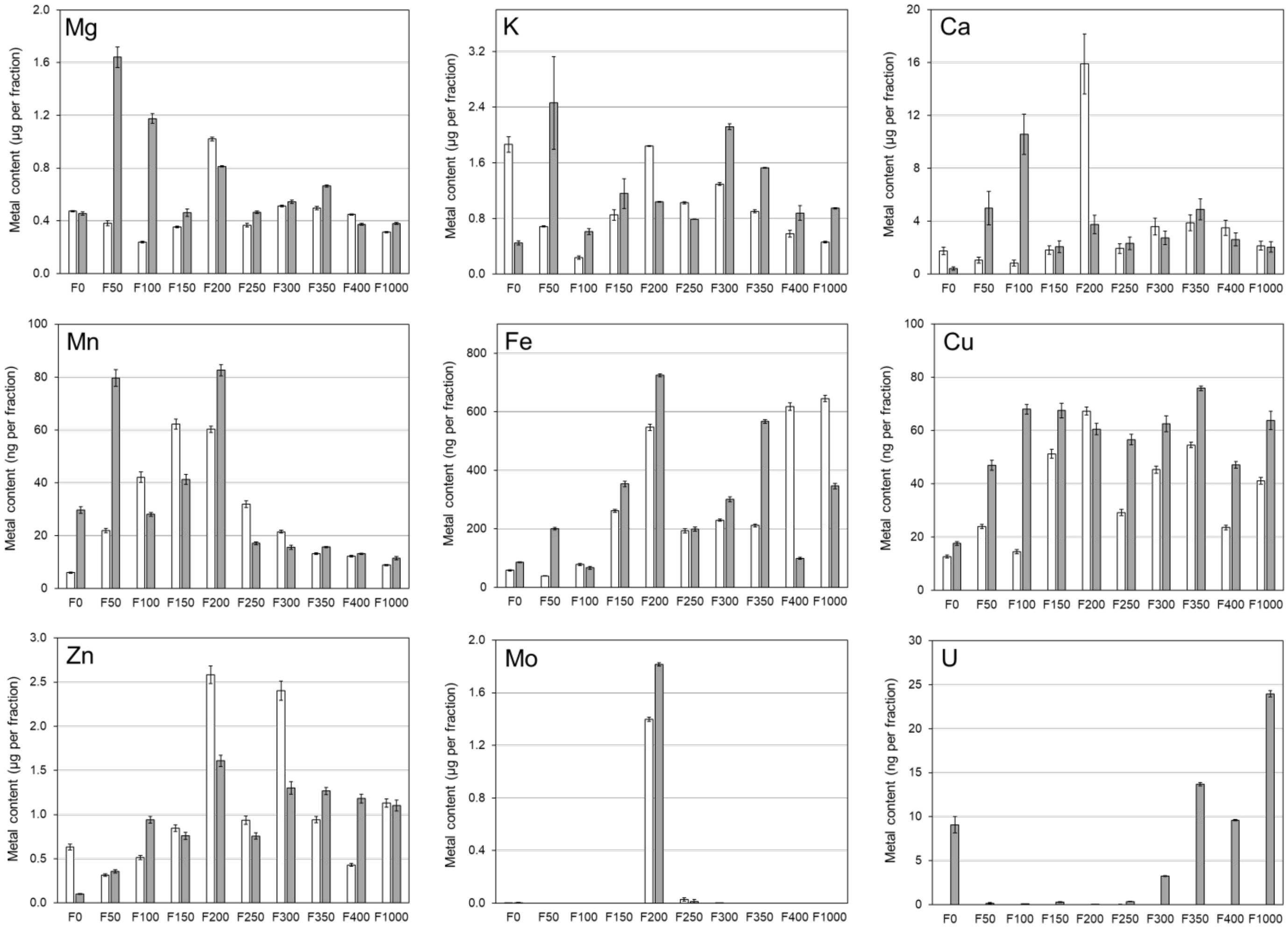

Figure 4: Elemental profiling in fractions from anion-exchange chromatography.
Soluble proteins (40 mg) from Arabidopsis cells grown for 24 h in the absence (U0) or presence of 50 µM uranyl nitrate (U50) were resolved by AEC on a Q-Sepharose column. Metals were extracted from proteins in 10% (v/v) nitric acid and analysed by ICP-MS. The elution profiles of each element in control (☐) and U-challenged cells (☐) are shown. Means ± SD for n=3 elemental analyses of representative AEC experiments.

Figure 5

Figure 5: Immunodetection of lysine and arginine methylated proteins in Arabidopsis cells challenged with U.
A- SDS-PAGE analysis of soluble proteins extracted from Arabidopsis cells grown for 24 h in the absence (U0) or presence of 50 µM uranyl nitrate (U50) and resolved by AEC on a Q-Sepharose column. Gel image for U0 is similar to the one from Fig. 2B, upper-right panel. B- Immunodetection of trimethyl-Lys in AEC fractions. C- Immunodetection of asymmetric dimethyl-Arg in AEC fractions. D- Closer views of SDS-PAGE and immunoblot for the fraction eluted at 100 mM NaCl. The band excised from the gel for MS/MS identification of Arg-methylated proteins is outlined in red. M, molecular mass markers, in kDa; T, total soluble extract; F0 to F1000, fractions eluted from the Q-Sepharose column from 0 (run-off) to 1000 mM NaCl.

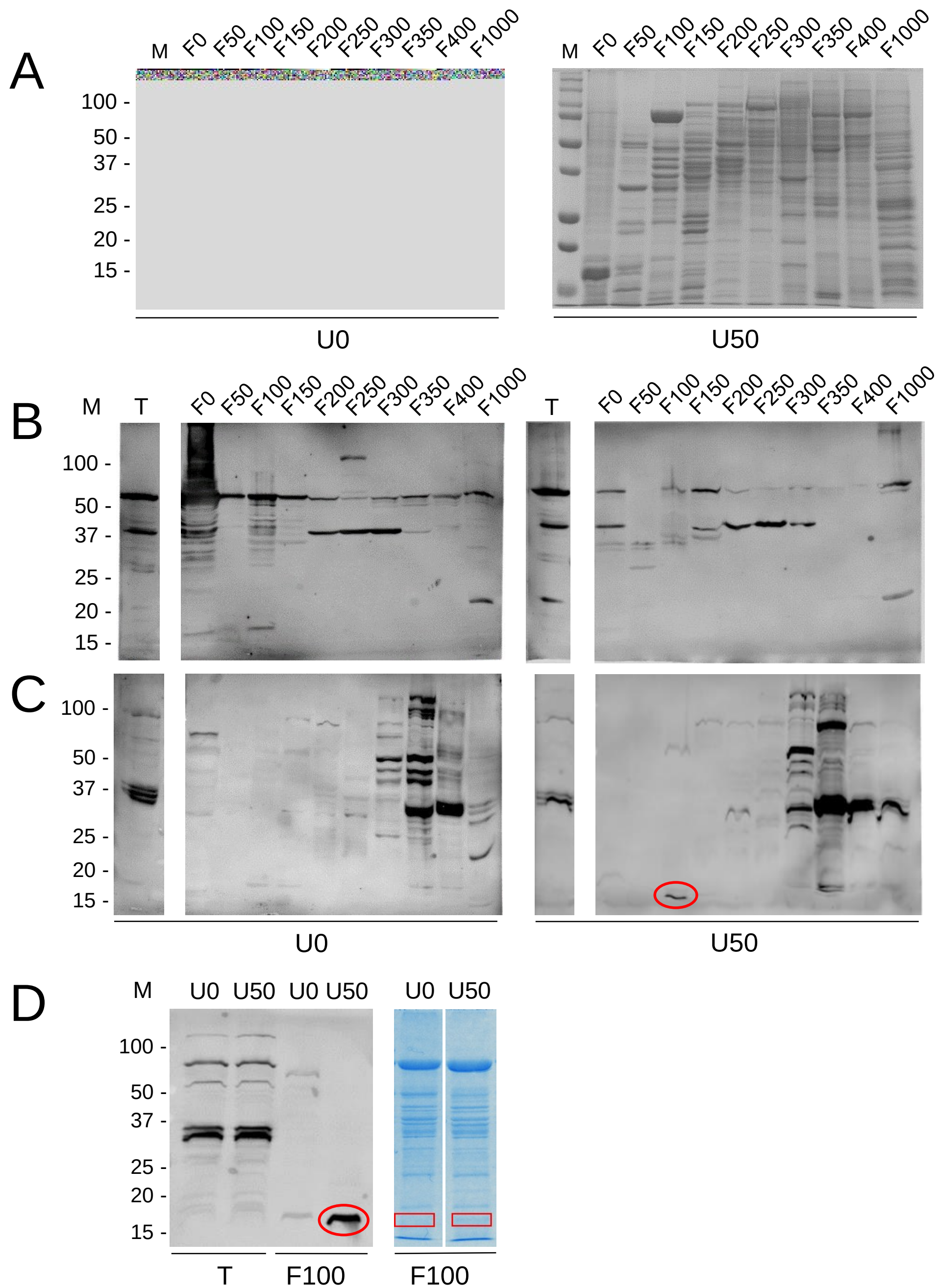

Figure S1

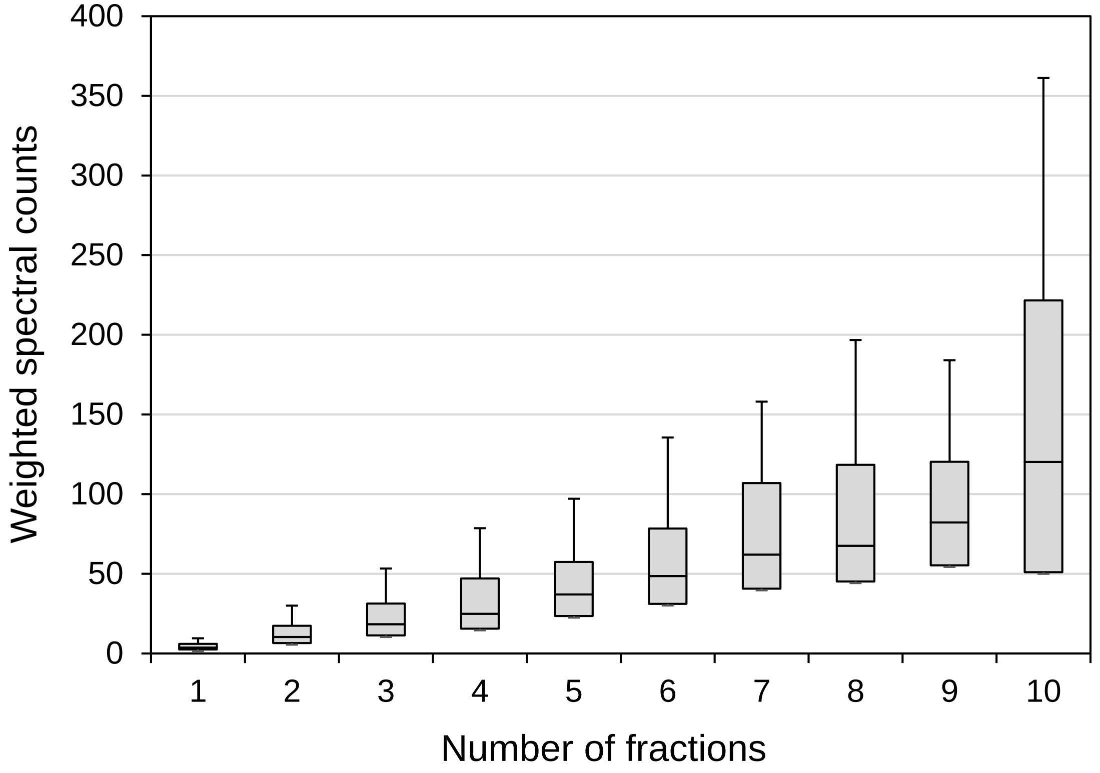

Figure S1: Influence of protein abundance on protein distribution in anion-exchange chromatography fractions.
The abundance of proteins identified by MS/MS was calculated using weighted spectral count (WSC) values. The higher the WSC, the more proteins were present in a large number of fractions.

Figure S2

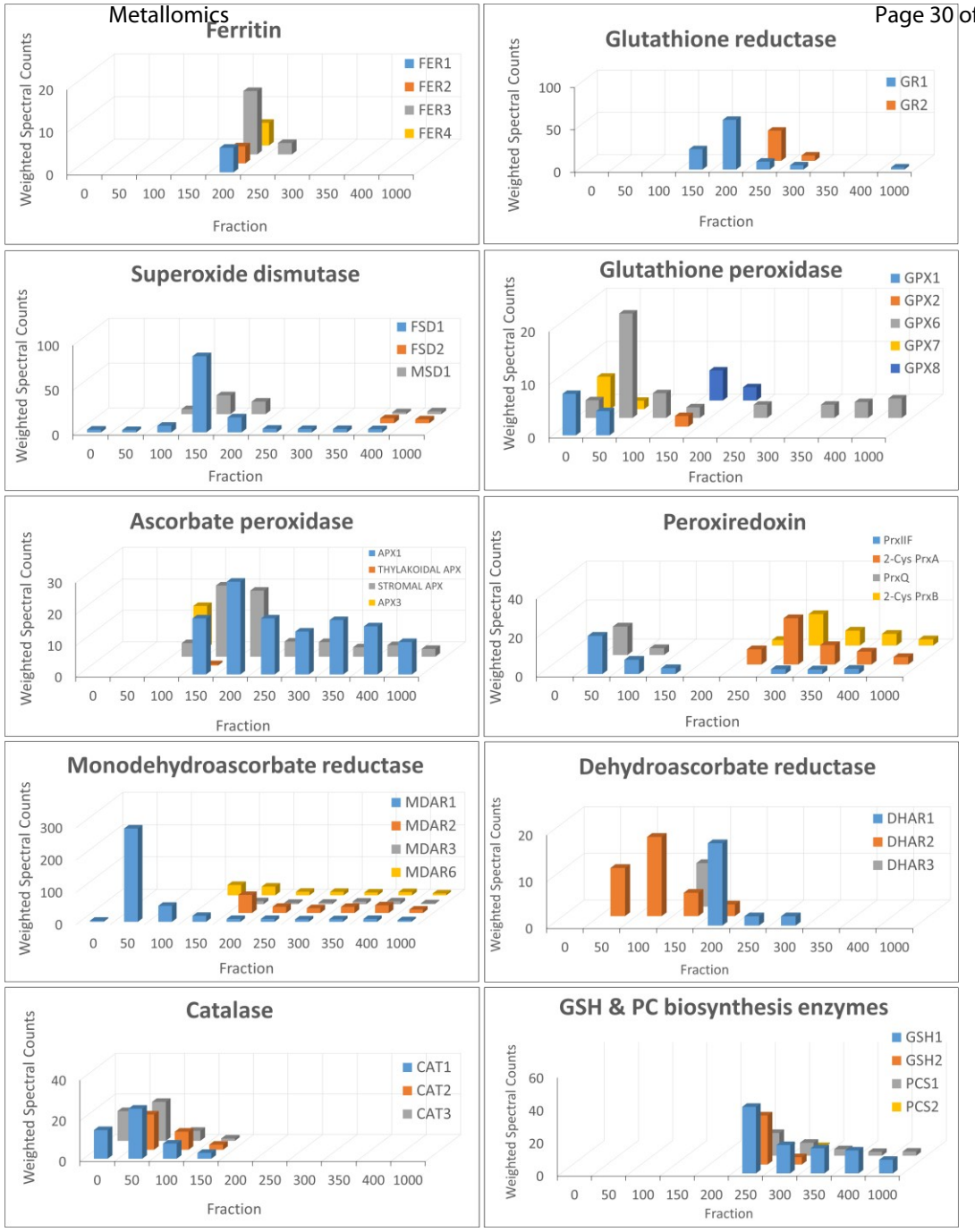

Figure S2: Elution profiles of metal- and stress-related proteins fractionated by anion-exchange chromatography. Some proteins involved in oxidative stress response and metal homeostasis were retrieved from MS/MS data and their elution profiles on Q-Sepharose were produced using WSC values.

Figure S3

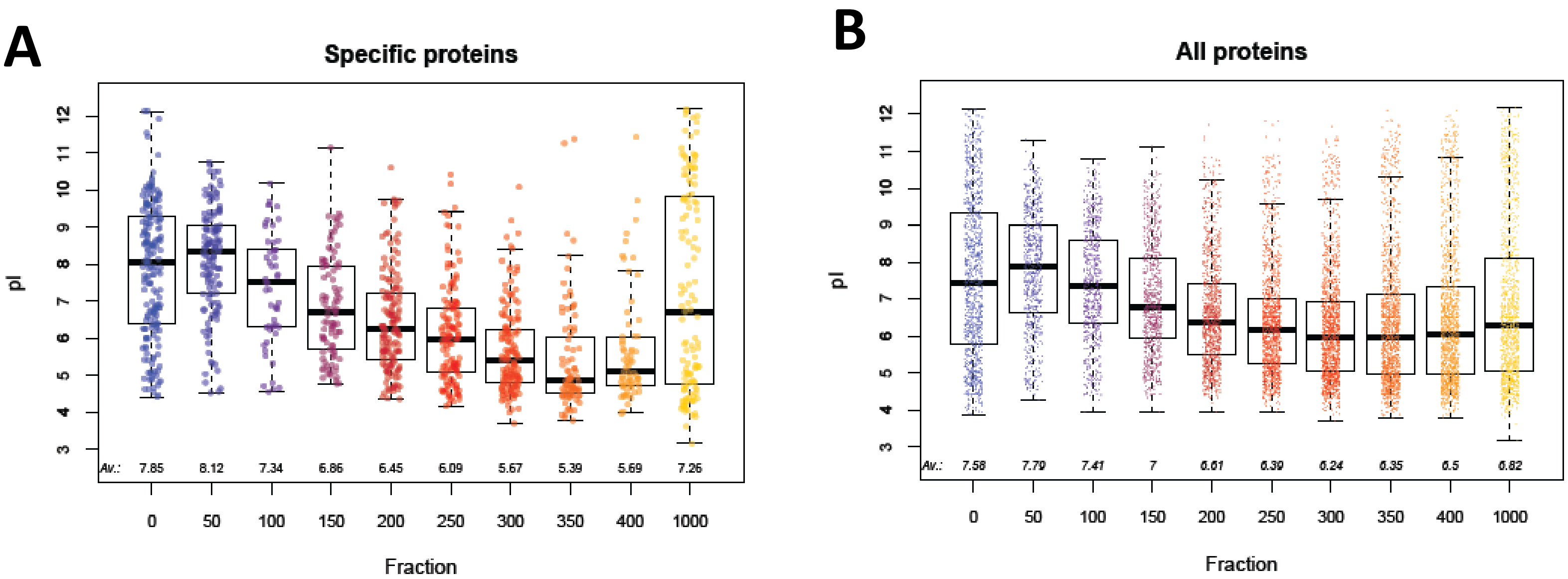

Figure S3: Influence of isoelectric point on protein distribution in anion-exchange chromatography fractions. Theoretical isoelectric points (pI) of full-length proteins were obtained from the TAIR database. A- Distribution of pI for specific proteins (eluted in a single fraction). B- Distribution of pI for all proteins. The average pI value for each fraction is indicated below boxplots.

Figure S4

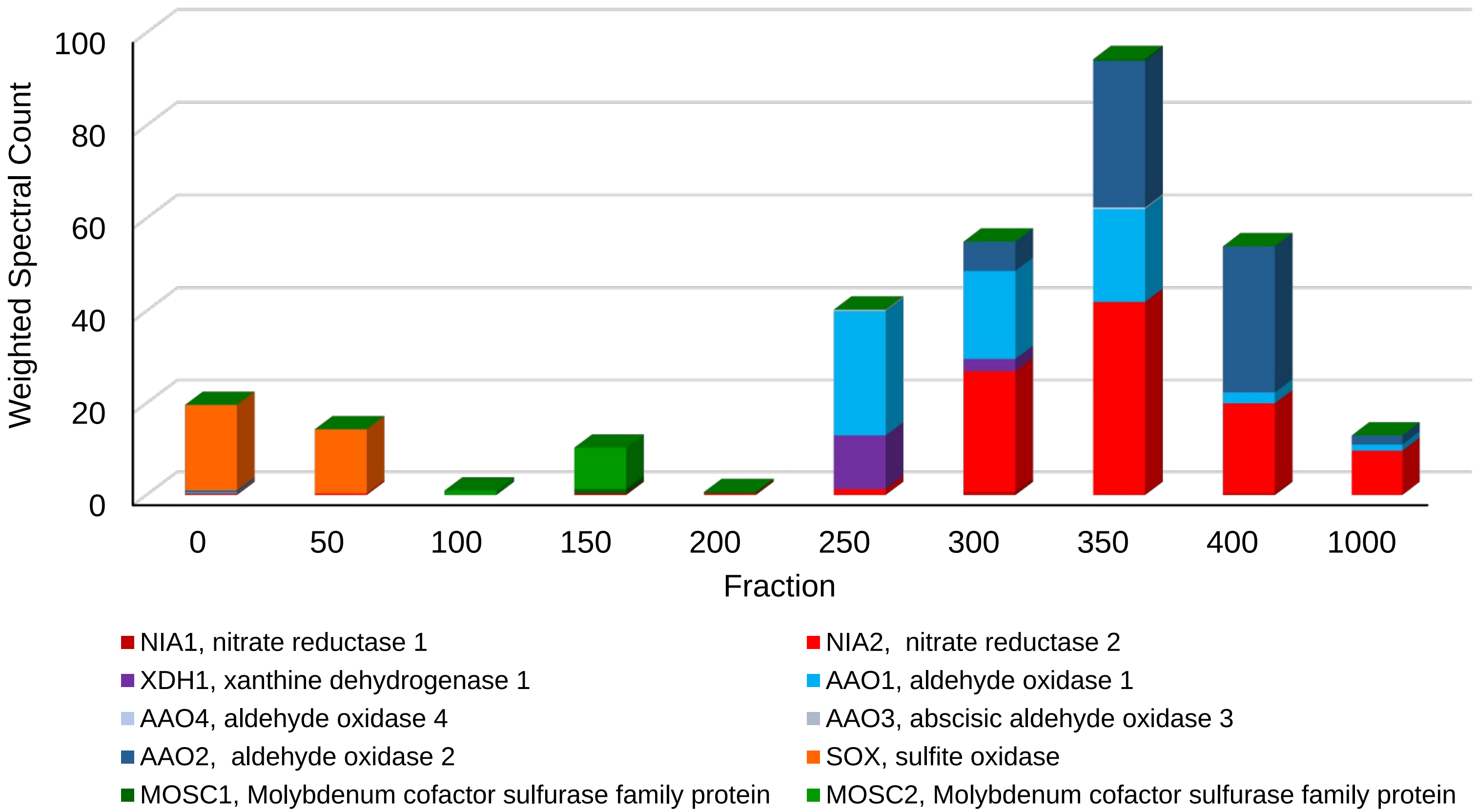

Figure S4: Elution profiles of MoCo containing proteins fractionated by anion-exchange chromatography. Molybdo-enzymes[63] were retrieved from MS/MS data and their elution profiles on Q-Sepharose were produced using WSC values.